# IV. 研究成果の刊行物・別刷

# Stochastic estimation of synaptic changes evoked by electrical stimuli in neural network in vitro

Tatsuya Haga, Osamu Fukayama, Takafumi Suzuki, Kunihiko Mabuchi
Graduate School of Information Science and Technology, The University of Tokyo

## 1.Introduction

Synaptic plasticity contributes to the process of memory and learning in the brain. However, measuring of EPSP as connection strength in large neural network has required great amount of time and work. In this paper, a novel way of estimating synaptic connectivities as a set of parameters of probabilistic neural network model has been developed. The parameters were identified to maximize the likelihood function by assuming spontaneous firings generated from the model. The method was evaluated with a simple simulated neural network, and applied to cultured cell network under electrical stimulus in a Multi Electrode Array Dish.

## 2.Method

We considered a firing probabilistic model represented by

$$p(x_t^{(i)}=1)=\mathrm{normcdf}(\sum_{j=1}^{N}\sum_{\tau=1}^{T} a_\tau^{(i,j,t)} x_{t-\tau}^{(j)}+\epsilon^{(i,t)},0,\sigma) \quad (1)$$

where $\mathrm{normcdf}(x,\mu,\sigma)$ is cumulative normal distribution function with random variable $x$, mean $\mu$, standard deviation $\sigma$. The number of neuron is $N$ and firing series $x_t^{(i)}$ is 1 when neuron $i$ fires at time $t$ 0 otherwise. synaptic weight at time $t$ from neuron $j$ to neuron $i$ in time-delay $\tau$ is $a_\tau^{(i,j,t)}$ . Here, $\epsilon^{(i,t)} = \xi^{(i,t)} - \theta^{(i)}$ where $\xi^{(i,t)}$ is the resting membrane potential of neuron i at time $t$ and $\theta^{(i)}$ is firing threshold of neuron $i$.

Log likelihood fuction for the model at time $t$ is

$$Q_t=\sum_{i=1}^{N}[x_t^{(i)}\log(p(x_t^{(i)}=1))+(1-x_t^{(i)})\log(1-p(x_t^{(i)}=1))] \quad (2)$$

$a_\tau^{(i,j,t)}$ and $\epsilon^{(i,t)}$ can be updated at each time using the gradient method to increase the log likelihood function . The update algorithm is

$$a_\tau^{(i,j,t+1)}=a_\tau^{(i,j,t)}+\mathrm{K}\frac{\partial Q_t}{\partial a_\tau^{(i,j,t)}},\forall i,j,\tau \quad (3)$$

$$\epsilon^{(i,t+1)}=\epsilon^{(i,t)}+\mathrm{K}\frac{\partial Q_t}{\partial \epsilon^{(i,t)}},\forall i \quad (4)$$

where K is the learning coefficient. The synaptic change was estimated in real-time with this method.

## 3.Experiments

### 3.1.Estimation in simulated network

The membrane potentials of four Hodgkin-Huxley neurons connected with synapses (Fig.1) are simulated for 20 minutes with a sampling rate of 10 kHz. For the first ten minutes, the EPSC of synapse from cell0 to cell1 was 80nA. During the next ten minutes i.e., 10-20min, this configuration was changed to 160nA. The firing series obtained was then analyzed with our method (K=0.8,$\sigma$ = 7). Results ($\max_\tau a_\tau^{(1,0,t)}$) are shown in Fig.2. Synaptic potentiation can be seen with convergence interval for about 100sec. The interval may make it difficult to estimate sharp synaptic change.

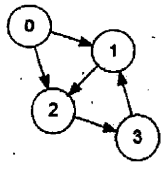


Figure 1: Simulated cell network (node:cell, edge:synaptic connectivity)

### 3.2 Application to neural network in vitro

We have built a system that can analyze synaptic changes in a neural network in vitro under electrical stimulus such as a single electrical pulse and "the 'Tetenus' " (high-frequency) pulse. The firing series obtained by spike sorting to voltages measured from 8 x 8 electrodes on a Multi-Electrode Array Dish was analyzed to estimate synaptic change. Fig. 3 shows the estimated network as a directional graph..

## 4.Discussion

While we have found that our method can be used to estimate synaptic changes, slow convergence speed may be a problem. The problem should be solved to apply our methods to various researches to to various researches such as quantitative evaluation of synaptic changes in neural networks in vitro under various conditions of electrical stimulli and in a rat brain with reward learning.

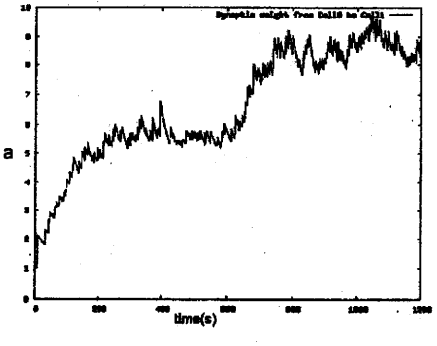


Figure 2: Estimated synaptic weight (cell 0 → 1)

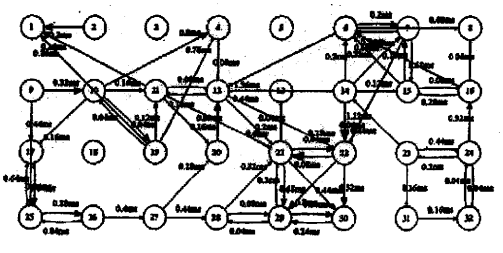

Figure 3: Estimated network

# A basic study of kinesthetic feedback by tendon vibration for prosthetic arms

Hiroaki Yaguchi, Kazuki Togawa, Osamu Fukayama, Takafumi Suzuki, Kunihiko Mabuchi
Graduate School of Information Science and Technology, The University of Tokyo

## 1. Introduction

Kinesthesia is crucial for precise control of the body. A loss of kinesthesia causes ataxia such as unsteadiness in gait and athetosis[1]. In the same vein, prosthetic limbs controlled by neural activities or myoelectric commands require proper kinesthetic feedback for precise control.

A transcutaneous vibration to a tendon non-invasively induces kinesthetic illusion. However, sensations of only small movements were evoked by vibrating a single tendon. We propose the use of a stimulation method in which both ends of each muscle are vibrated to evoke sensations of larger movements.

## 2. Methods

Twelve healthy volunteers participated in the experiment. Each participant was seated on a chair and held both arms on support tables (Fig.1). The tendons of right biceps brachii and extensor digitorum were vibrated at a frequency of 100 Hz and a peak-to-peak amplitude of about 1 mm. Participants were instructed to show movement velocity they felt in their right arm by moving their contralateral left arm. The intensity of evoked kinesthesia was calculated by subtracting the angular velocity of the right arm from that of the left arm.

### 2.1 Vibration to biceps brachii

The vibration was presented to both ends of the biceps of 8 participants. While the distal vibration was applied to the tendon, the proximal vibration was applied to the muscle near the muscle-tendon junction because the proximal tendons were behind the other muscles. Vibrations to distal tendon and/or the proximal end were performed 10 times in a random order for a total of 30 trials per participant.

### 2.2 Vibration to extensor digitorum

The vibration was presented to the distal and proximal tendons of the extensor digitorum of 9 participants. Vibrations to distal and/or proximal tendon of the muscle were performed 10 times in a random order for a total of 30 trials per participant.


Fig. 1 Experiment. Tendons of right arm were vibrated. Participants moved their left arm to show the velocity of the movement they felt in their right arm.

## 3. Results and Discussion

Compared to vibration to the distal tendon or proximal end of biceps, vibration to the both evoked a sensation of larger movement ($\alpha = 0.05$, Fig. 2). Similarly, vibration to the both tendons of extensor digitorum evoked a sensation of larger movement than that to the distal or proximal tendon ($\alpha = 0.05$, Fig. 3).

These results may be caused by increasing activity of Ia afferents from the vibrated muscle. Fallon et al.[2] found that only 6 of 32 Ia afferents generated an action potential per cycle when a single tendon was vibrated. Vibration to both ends of a muscle may activate Ia afferents more than that to one end.

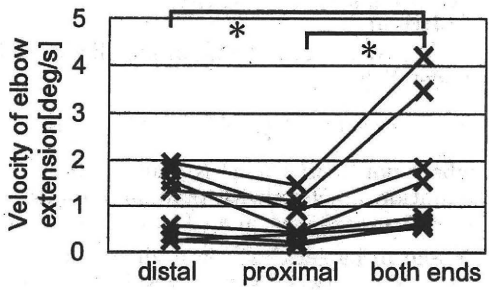


Fig. 2 Mean velocity of illusory movement induced by vibrating biceps. (*: $p<0.05$)

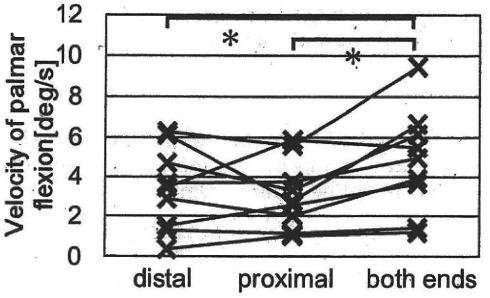


Fig. 3 Mean velocity of illusory movement induced by vibrating extensor digitorum. (*: $p<0.05$)

## 4. Conclusion

We proposed the use of a stimulation method in which both ends of a muscle are vibrated to evoke sensations of larger movement. Vibration to both ends of biceps or extensor digitorum evoked a sensation of a larger movement than that to a single tendon.

## 5. References

[1] A. Sghirlanzoni, D. Pareyson and G. Lauria, "Sensory neuron diseases," *The Lancet Neurology*, 4, 2005, pp.349-361.
[2] J. Fallon and V. Macefield, "Vibration sensitivity of human muscle spindles and golgi tendon organs," *MuscleNerve*, 36, 2007, pp.21-29.

## 6. Keywords

kinesthesia, tendon vibration, non-invasive stimulation

# 慢性神経信号計測に向けた針型電極の自動位置制御の基礎的検討

柴本 浩児　深山 理　鈴木 隆文　満渕 邦彦
東京大学大学院　情報理工学系研究科

Basic study of automated high-speed positioning of neural electrodes for chronic recording

K.SHIBAMOTO, S.FUKAYAMA, T.SUZUKI, K.MABUCHI,
Graduate School of Information Science and Technology, The University of Tokyo

［はじめに］ブレイン・マシン・インタフェース (BMI) の実用化に向けた重要な課題として、慢性計測における神経信号の安定的な取得が挙げられる。多くの BMI では、脳に針型の神経電極を刺入して計測を行うが、対象の自由行動に伴う衝撃や振動によって電極と脳との相対的な位置関係がずれ、当初計測できた信号を失ってしまうことが問題となっている。本研究では、針電極の埋め込み深さを高速に自動制御することによって、複数の神経細胞と電極との相対的な位置変動に追随可能な慢性計測系の構築を試みる。

［電極埋込深さに応じたスパイク振幅の変化特性］まず予備実験として、ラット海馬に針型電極を刺入し、埋め込み深さに応じた神経発火波形の平均振幅の変化を観察した。その結果、特定の深さに対して再現性良く振幅が最大となり、細胞に最も近接したことが示唆された (Fig1)。

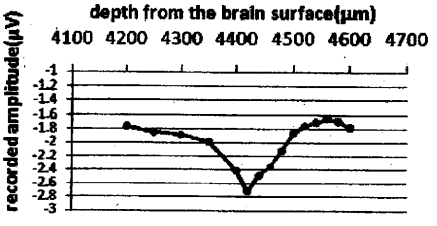


Fig 1: 深度を変化させた時のスパイク平均振幅

［提案手法］前節の予備実験により、計測されるスパイク振幅が連続的に増大するように電極深さを逐次調節することで、電極を神経細胞の近傍に保持できるものと考えられる。複数の神経細胞由来のスパイクが得られる状況 (マルチユニット計測) においては、それぞれの平均高さが指標となりうる。以上を踏まえ、以下のアルゴリズムに従い電極深さを変化させることとした。1) 初期位置からスパイクを取得した後、主成分分析を施し、クラスタリングを行う。2) クラスタ中心に最も近い波形をテンプレートとする。3) 近傍点を $\pm 2[\mu m]$ とし、そこで得られたスパイクに対してテンプレートマッチングを行う。弁別されたそれぞれのスパイクグループに対し、Negative peak の平均値 $A_i (i = 1, 2, ...)$ を求める。4) 評価関数 $J = \sum_{i=1}^{N} A_i$ が前回よりも小さくなっていた場合、それぞれのテンプレートを得られた平均値と一致するような比率で更新し、3) に戻る。それ以外の場合は、何もせず 3) に戻る。ただし、解の探索においては焼きなまし法により局所解を回避した。

［評価実験］ここでは、計算機シミュレーションにより上記アルゴリズムの妥当性を検討した。電極付近の神経細胞を 2 個と設定しそれぞれの深さを 4450$\mu$m、4500$\mu$m、電極刺入軸との距離を 50$\mu$m、60$\mu$m とした (Fig2(a))。実験に用いるデータ列は以下のようにして生成した。まずラット海馬から得られた神経スパイクを 2 種類取得し、それぞれ 30〜40Hz、5〜15Hz の頻度で距離の二乗に反比例した振幅で発火させた。次にノイズ用としてスパイクを 50 種類取得し、振幅を 1/8 にした後に 30〜40Hz の頻度で発火させる。深さ 4510$\mu$m を初期位置として探索を開始したところ、その推移は Fig2(b) となった。ここで、実線は電極の位置、点線は $J$ が最小となる位置を示す。

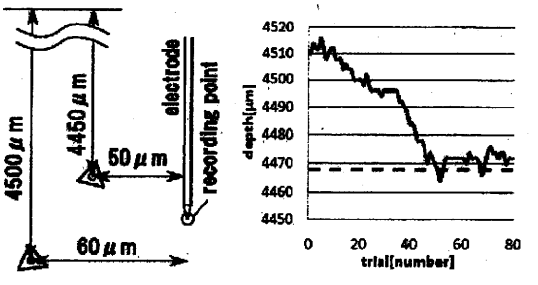


(a)　(b)

Fig 2: シミュレーション

［おわりに］電極と細胞の位置関係によってスパイク振幅の大きさが異なるという予備実験での考察を基に、評価関数を最小にするように電極位置を動かすアルゴリズムの提案を行った。その結果、複数の神経細胞を弁別しながら評価関数が十分に小さくなる位置まで移動することが可能であることが確認できた。今後は、このアルゴリズムの改良と実データでの検証が必要である。

# Study on detection and induction of plastic changes in rat brain while connected with a vehicular BMI RatCar

Osamu Fukayama, Takuya Kohama, Takafumi Suzuki, and Kunihiko Mabuchi
Graduate School of Information Science and Technology, The University of Tokyo

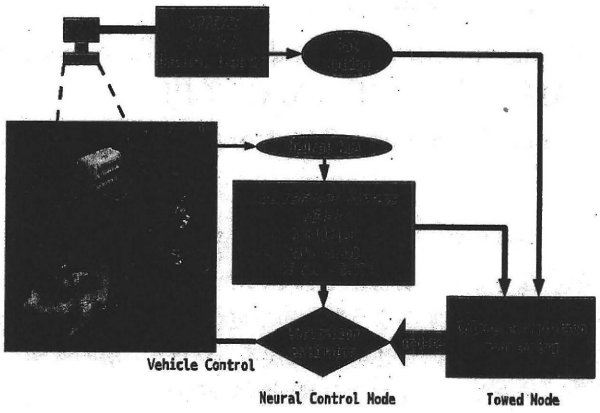


Figure 1: RatCar System operated in 2 modes; neural control mode and towed mode.

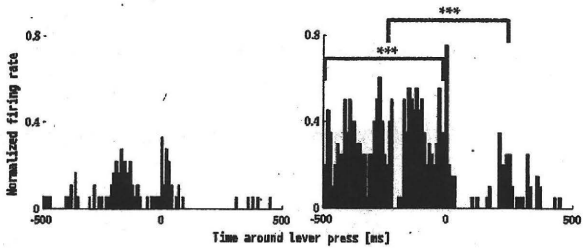


Figure 2: Normalized neural firing rate observed around lever pressing. Pre-stimulation stage (left) and post-stimulation stage (right).

## 1. INTRODUCTION

Brain-machine interfaces (BMI) are promising to provide a new method for device controls. However, brain activities are known to show plastic changes, which disturbs correlating them to a specific motor command. On the other hand, the brain plasticity may assist developing BMIs by adapting the brain with simple neural decoding algorithms which do not initially describe proper neural commands. A vehicular BMI for a rat, which we call "RatCar", has been developed to observe and induce those plastic changes.

## 2. METHODS

A soft neural electrode made of parylene polymer which had 4 gold recording sites was implanted in the motor cortical regions related to forelimbs of a rat. They were applied to two experiments; controlling a vehicular brain-machine interface ("RatCar"), and forcibly correlating neural activities with a specific action by inducing plastic changes with electrical intercortical micro-stimulation (ICMS).

### 2-1. Vehicular BMI Control

The RatCar system consists of the neural electrodes described above, an optical motion tracker, locomotion estimators installed on a personal computer, and a vehicle body (Fig. 1).

The system were designed to operate in two modes; "neural control" mode and "towed" mode. In the neural control mode, the vehicle was driven according to extracellular multiunit activities (MUA) patterns recorded from a rat. The rat was suspended under the vehicle as its limbs gently touched the ground. In contrast, in the towed mode, the vehicle was pulled by a rat locomoting with its natural limbs. MUA patterns from the rat brain and motion of the vehicle were simultaneously acquired to identify correlations between the variables. The update process repeated every 100 ms.

### 2-2. Correlation Forcing

A study to forcibly correlate neural activities near electrodes with a specific motion in an action learning chamber. First, a rat with neural electrodes implanted in its forelimb region of the motor cortex was trained to push a lever to gain food rewards. Then, a channel was chosen which had initially no strong correlation with the motion (i.e., lever pushing), and ICMS was applied to the channel to induce correlation with the lever pushing motion.

All the experiments we performed followed guidelines given by the "Animal Experiments Committee of the University of Tokyo".

## 3. RESULTS

The vehicular BMI system operated online; (a) determining vehicle motion in the neural control mode, and (b) monitoring the correlation between neural activities and locomotion of the rat in the towed mode. Properties of those correlations and determination results depended on incidentally recorded neurons.

Then, the correlation forcing method was applied. Normalized neural firing rates increased in prior to lever pushing by the ICMS (Fig. 2), which resulted in stronger initial correlation between a recorded neurons and motor commands related to limb control.

Combination of those methods are promising to detect and apply brain plasticity for a precise BMI.

## 4. KEYWORDS

Brain-machine interface, Brain plasticity, Locomotion estimation, Extracellular recording, Rat

# Development and characterization of flexible L-glutamate biosensor

Naoki Kotake, Takafumi Suzuki, Osamu Fukayama, Shoji Takeuchi, Kunihiko Mabuchi
The University of Tokyo

## 1. INTRODUCTION

One of the main excitatory neurotransmitters in the mammalian brain, L-glutamate (Glu), is involved in most aspects of normal and abnormal brain function. Previous studies have reported several types of sensors that detect the concentration of Glu in the brain. These sensors consist of a rigid material such as silicon or ceramic [1-2], which does not deform in the brain and consequently damage surrounding tissues when the body moves. We propose the use of a flexible sensor that can fit the brain.

## 2. METHODS

***Sensor fabrication.*** We used MEMS technology to fabricate the sensors that consist of a parylene thin film structure and four-channel recording sites. A gold layer was deposited and patterned on the first parylene layer. The structures of sensors were then defined by oxygen plasma etching after second parylene layer deposition. After peeling the sensor from the wafer, Nafion was coated on each recording site to repel anions such as ascorbic acid. Glutamate oxidase (GluOx) was immobilized onto the surfaces of two recording sites by coating with bovine serum albumin (BSA) and glutaraldehyde. Others were coated with BSA and glutaraldehyde mixture without GluOx. The sites immobilized by GluOx and ones coated with only BSA worked as Glu detectors and control sites, respectively.

***Electrochemical measurements.*** Detection tests of Glu concentration were done in vitro using constant-potential amperometry. We used a fabricated sensor, a platinum counter electrode, and an Ag/AgCl reference electrode. These electrodes were placed in a continuously stirred 0.1 M phosphate buffered solution (pH 7.4, 37 °C), and operated the sensor at a constant potential of +0.7 V vs. Ag/AgCl reference electrode.

## 3. RESULTS

A raw current-time response of the fabricated sensor is shown in Figure 1. We consecutively injected Glu using a micro-pipette at the points of time indicated by the arrows (final concentration

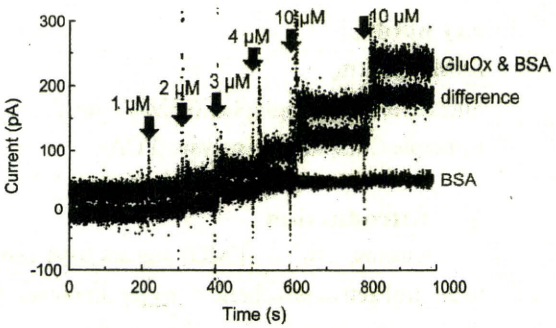


Fig. 1. Response for consecutive Glu injections.

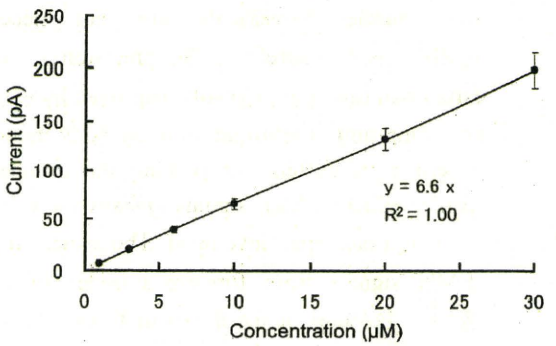


Fig. 2. Calibration curve of sensor.

was 30 μM). The response of the sensor was stable and the response time was within 20 s. The current response of sensor showed the linear response to Glu concentration in the whole measurement range (Fig. 2). The sensor sensitivity calculated from the slope was 6.6 pA/μM, and the linearity ($R^2$) was 1.00 (n=8).

## 4. CONCLUSION

We proposed and fabricated a flexible microsensor for detecting the concentration of Glu. The results of in-vitro measurement show that the sensor showed good linearity in the calibration test and could be used at a concentration of under 30μM Glu.

## 5. REFERENCES

[1] O. Frey, et al., Conf. Proc. IEEE Eng. Med. Biol. Soc., pp. 6040-6043 (2007)

[2] J. J. Burmeister et al., J. Neuroscience Methods 119, p. 163-171 (2002)

## 6. KEY WORDS

Flexible, sensor, L-glutamate, Neurotransmitter, Parylene

# Estimation of finger movements by electromyographic signals with external triggers for playing trumpet

Yutaro Kobayashi, Osamu Fukayama, Takafumi Suzuki, Kunihiko Mabuchi
Graduate School of Information Science and Technology, The University of Tokyo

**Key words**
Prosthetic arm,
Surface electromyographic (sEMG) signals,
Principle Component Analysis (PCA)

## 1. Introduction

Electromyographic (EMG) signals have been used to control active prosthetic arms for amputees. One of the obstacles in achieving such prosthetic arms is the *timed estimation of posture*, because EMG signals and muscle movements are not necessarily synchronized. Therefore, the precision of posture estimation can be remarkably improved by externally providing timing information using body motion. An experimental system for playing the trumpet with surface EMG (sEMG) signals to show the validity of our claim has been developed. The system recorded sEMG signals from forearm muscles of trumpet players. Postures of the hands that push the trumpet valves were estimated using the sEMG signals while the correct timing in which the valves were pushed was provided externally.

## 2. Method

### 2.1 Valve patterns of trumpet

Trumpet players make different pitches by pushing the 3 valves in different patterns. The 2nd finger controls the 1st valve (the valve closest to the mouthpiece), and the 3rd and the 4th finger control the 2nd and 3rd valve respectively. There are 7 patterns in which the valves are musically allowed to be pushed. Surface EMG signals was recorded to estimate the postures of the three fingers. The correct timing in which the valves were pushed was also recorded (*timing given externally*).

### 2.2 Onset detection methods

*Selected threshold-based onset detection methods* [1] were used to estimate the timing of the valves pushed from sEMG signals. The results were then used to compare with the *timing given externally* (Section 3).

### 2.3 Feature extraction

Surface EMG signals from 8 electrodes were applied to the subject's right forearm (flexor and extensor muscles), and recorded with the sampling rate of 25kHz. 0.16 second of data, right before the valves were pushed, was extracted. Covariance Matrices were then calculated and used as features.

### 2.4 Experiment

Four different subjects were asked to push the valves with the following instructions.

(A) push 1st valve *10 times (Fig. 1 color: black)
(B) push 2nd valve *10 times (Fig. 1 color: red)
(C) push 3rd valve *10 times (Fig. 1 color: green)

## 3. Results and Discussion

The Features of the sEMG signals were investigated by Principle Component Analysis (PCA). Fig. 1 (left) shows the results of a subject analyzed using the timing given externally. Fig. 1 (right) shows the results of the same subject analyzed using the timing estimated by Onset detection method (2.2). These results illustrate the effectiveness of providing timing externally to estimate the postures of the hands.

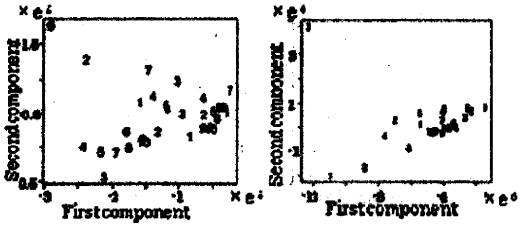


Fig. 1:PCA (left:timing is given externally, right:onset detection method)

*Numerical show the order in which the valves were pushed in each experiment.

**Reference**

[1]Staude G. et al.:"Onset Detection in surface electro myographic signals," Proc. Journal on Applied Signal Processing, Volume2, pp.67 – 81,2001

# 感覚神経系障害患者のための
# ウェアラブル感覚補填・感覚強化システムの開発
## ～マイクロスティミュレーション法による触圧覚生成と感覚増強～

# Wearable sensory prosthetic system for patients with sensory disturbance
## -generation of somatic sensation and its enhancement using microstimulation method-

○新納 弘崇 (電通大)　國本 雅也 (済生会横浜市東部病院)　鈴木 隆文 (東京大)　満渕 邦彦 (東京大)　下条 誠 (電通大)

Hirotaka Niiro(UEC),Masanari Kunimoto(Saiseikai Hosp.),Takafumi Suzuki(Univ. of Tokyo),
Kunihiko Mabuchi(Univ. of Tokyo),Makoto Shimojo(UEC)

**Abstract**— In this study, we attempted to develop a prototype of a wearable sensory prosthetic system with which patients suffering from peripheral sensory disturbance will be able to feel somatic sensations as if they were touching an object with their healthy and intact hand. The system consists of finger sacs and palm patch equipped with flexible pressure sensors, and micro-electrical stimulation of the sensory nerve fibers was used in order to evoke somatic sensations. The results showed that the system worked satisfactorily, and it is demonstrated that the system will be able to compensate or even enhance sensory function of the patients with sensory neuropathy.

**Key Words:** sensory feedback,intelligent prosthetic hand,work support,microstimulation method

## 1. 緒言

病気や事故によって感覚を失ってしまった場合，日常生活に多大な支障をきたす事になる．そこで，障害によって失った感覚を回復するための一つの方法として，感覚神経電気刺激を利用した感覚を提示する研究がなされるようになった [1].

実際の生体では，感覚受容器が受けた刺激を活動電位のパルス列に変換し，中枢に伝達されることで感覚を得る [2]. そして，刺激を伝える感覚神経線維に同じ活動電位列を発生させることができれば，実際に刺激を受けた時と同じ感覚を得ることができる.

そこで本研究では，触覚センサの情報をマイクロスティミュレーション法を用いて，感覚神経経由により触感覚として提示するシステムの開発を目的とした.

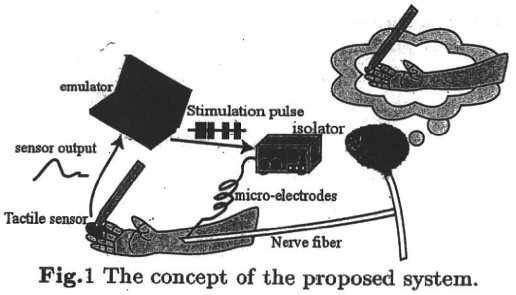


**Fig.1** The concept of the proposed system.

## 2. 実験システム

実験システムの全体構成を図 2 に示す．システムは触覚センシングと神経線維インターフェースの 2 つに分かれている．前者は被験者の指先に装着した触覚センサの情報をコンピュータに取り込み，後者は取り込んだ情報に応じて神経線維を刺激するパルス列を出力する．以下各実験システムについて説明する.

### 2.1 触覚センサ

触覚センサとして FingerTPS(PPS 社製) を用いた．センサは人の手に装着し，接触力を検出するフレキシブルな静電容量型圧力センサである．出力は Bluetooth 通信で PC に接続され，40Hz で更新する.

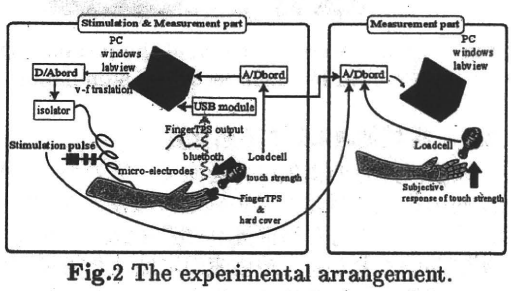


**Fig.2** The experimental arrangement.

### 2.2 神経線維インターフェース

触覚センサからの情報を基にマイクロスティミュレーション法を用いて感覚を被験者に提示する．マイクロスティミュレーション法とは，経皮的に微小針電極を感覚神経線維の中に刺入し，電気刺激パルス列を入力することで，人工感覚を生成する手法である.

**Fig.3** The Finger TPS system.

**Fig.4** The manner in which microstimulation is performed.

## 3. 感覚提示実験

感覚神経への電気刺激によって生成される圧感覚の強度はパルス頻度に依存している [3] 事が報告されており，本研究ではこの関係を応用する．

### 3.1 実験目的・方法

本実験の被験者は，健全な男性 1 名である．被験者は座っており，開眼状態で実験を行った．指先に加えた力によって発生する感覚と等価な感覚量を感覚神経の電気刺激で発生させることを目的とする．この為には，指先に発生した感覚を定量評価する必要がある．今回我々は生成された感覚の計測法として，加圧した指先に発生される力と反対の指先でその力に対し等価な感覚量を提示させることとした．

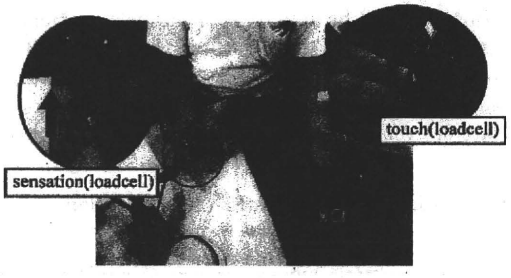


**Fig.5** Quantitative evaluation of the pressure sensation evoked by microelectricqal stimulation.

### 3.2 機械刺激に対する感覚量

まず，片方の指先に力を加え，その力と同等の力を反対の指先で提示する実験を行った．実験結果を図 6 に示す．加圧力と感覚量の相関係数は 0.98 であり，相関が高いことから，皮膚表面に加えた機械刺激と感覚量の関係はほぼ等価な関係であることが示された．

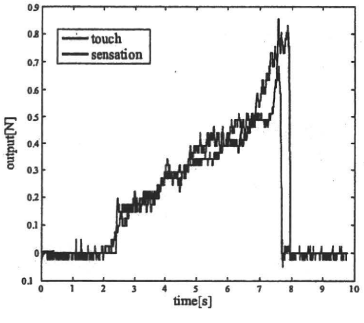


**Fig.6** Actual force applied to the TPS sensor and the subjective magnitude of the evoked pressure sensation.

### 3.3 電気刺激に対する感覚量

次に，指先にハードカバーを装着し，感覚を遮断した状態で感覚を提示する実験を行った．FingerTPS の出力をパルス列頻度に変換・出力し，マイクロスティミュレーション法によりパルス列を神経に伝達することで感覚を提示した (図 7)．

本実験では，圧覚から電気刺激のパルス列頻度への変換式は，FingerTPS の出力 $x$ を係数 $a$ にて整数倍し，これをパルス頻度の周波数 $f$ とした．即ち，$f = ax$ で，本実験では $a = 50$ とした．

**Fig.7** The manner in which a subject enhances somatic sensations by the developed system.

実験結果の一例を図 8 に示す．グラフは上から FingerTPS と加圧力と感覚量，出力周波数，出力パルスである．実験結果をみると，パルス頻度が増加することによって被験者の感覚量は増加している．押付力と感覚量の関係は相関係数 0.91 であり，高い相関があることから被験者の感覚を生成出来ていることがわかる．また，FingerTPS と押付力との相関係数は 0.97 であり，FingerTPS が接触力を忠実に再現出来ていることが確認できる．

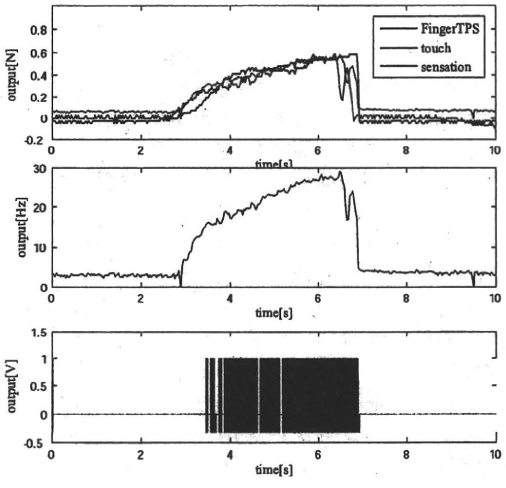


**Fig.8** Response of subjective pressure sensation evoked by the microelectrical stimulation, pulse train for the microelectrical stimulation, and the actual force applied to the Finger TPS system,

## 4. 結言

触覚センサの出力をマイクロスティミュレーション法により神経フィードバックし，人工感覚を提示するシステムを構築した．触覚センサの出力をパルス変換し，マイクロスティミュレーション法により提示することで失われた感覚を補綴しうる可能性を示した．

## 文 献

[1] M.Shimojo,T.Suzuki,A.Namiki,T.Saito,M.Kunimoto, R.Makino,H.Ogawa,M.Ishikawa,K.Mabuchi "Development of a system for experiencing tactile sensation from a robot hand by electrically stimulating sensory nerve fiber" IEEE Trans.Robotics and Automation(CD-ROM),2003

[2] Kandel,Schwartz,Jessell"PRINCIPLES OF NUERAL SCIENCE Fourth Edition",McGraw-Hill,2000

[3] T.Suzuki,K.Mabuchi,H.Nishimura,T.Saito,N.Kakuta, M.Kunimoto,M.Shimojo,The Relationship between Stimulation Signals and Subjective Intensities and Areas, Proc. Int. Conf. of the IEEE EMBS,Atlanta, 459, Oct. 1999.

# Linking human nervous system with mechanical control system of next-generation artificial organs

Kunihiko Mabuchi
Graduate School of Information Science and Technology, The University of Tokyo

## １．はじめに

近年、生体の神経系と機械系の情報ラインを直接接続し、運動神経系の情報によって義肢などの外部機器を制御したり、逆に、求心性の感覚神経系に外部から刺激を入力する事によって、人為的に感覚を発生させたりする所謂ブレイン・マシン・インタフェース（ＢＭＩ）システム、或いはブレインコンピュータインタフェース（ＢＣＩ）システムとか呼ばれるシステムの開発が盛んに行われるようになってきているが、次世代の人工臓器や人工器官では、これらの技術を用いて生体の神経系と人工臓器・人工器官を直接結んだシステムを開発していく事が大きな目標となって来るであろうと思われる。

神経系には大別して遠心性の運動神経系・自律神経系と求心性の感覚神経系とがあるが、遠心性の神経系と外部機器を接続するいわゆる出力型のＢＭＩシステム（人工臓器）としては、運動神経系では、随意運動機能を持つ義肢が典型的な例であり、また、自律神経系に関しては、交感神経系の活動や副交感神経系の活動情報によって、最適な条件で作動する人工心臓システムなどがその例として挙げられる。

一方、求心性の感覚神経系と人工の感覚器（センサ）を接続する、いわゆる入力型ＢＭＩ（人工感覚器）に関しては、人工聴覚（人工内耳）は臨床的に最も成功しているＢＭＩシステムであり、すでに 30 年間の歴史と 10 万人以上の患者を持つ確立した治療法となっている。また、人工視覚もまだ実験段階ではあるが、多くの施設で研究が進められてきており、人を対象とした実験も行われつつある。

このような、所謂ブレイン・マシンインタフェースシステムの急速な発展は、近年における脳科学の進展や MEMS（micro-electromechanical system）技術の進歩を背景としたものであるが、DARPA（米国の国防省国防高等研究計画庁）等、軍事関係の組織が非常に大きな予算を投入してプロジェクトを推進して来た事も関与している。また、マスコミでは、いわゆる「光」の面を中心に取り上げる事もあり、あたかも（一般には）明日にでもこのような技術が実現するかのような印象が抱かれちであるが、人工臓器・人工器官の領域でＢＭＩシステムを実際の臨床に耐えうる段階まで進めるには、電極の開発やコーディング・デコーディング則の解析など、まだ多数の問題点が残っており、これからも長い期間と地道な努力が必要ではないかと考えている。

## ２．電極を中心とした諸問題点について

先に挙げた問題点の中で、最大のものは、神経系と機械系の間で情報の入出力をどのように行うかという手法の問題であり、これには、１）非侵襲的手法によるか、侵襲的手法によるか、２）情報の入出力を何処で行うか、などの側面がある。神経活動の非侵襲的計測法としては、現在、脳波（EEG）、脳磁図（MEG）、機能的 MRI（fMRI）、近赤外スペクトロスコピー（NIRS）などが試みられているが、得られる情報量や空間分解能、リアルタイム性に問題が有り、現在は精細な義手の運動制御や感覚生成を行おうとする場合には、主に金属ワイヤ電極や剣山型電極などを直接神経系に刺入し、計測・刺激を行う侵襲的方法が主流で、その他、開頭はするが、刺入は行わず、柔軟なシリコンなどで出来たシートに電極アレイを配置した所謂 ECo-G（皮質電図）電極を硬膜下に留置して低侵襲的に local field potential の計測や刺激を行う試みも多数行われている。

情報の入出力を行う部位としては、中枢神経系（脳）と末梢神経系があるが、極端にいえば、脳の機能が侵されずに残存していれば、同部位にアクセスする事によってほぼ全ての病態に対応する事が可能で、形態的にもアクセスしやすいため、大脳皮質が多く用いられるが、万が一、感染や組織の損傷などの合併症が発生した場合の危険性を考えると、末梢神経でのアクセスの方が有利な面もある。侵襲的手法で用いる電極に関しては、昔から用いられる金属ワイヤ電極や針電極をベースにしたもの、ＭＥＭＳ技術をベースにしたプローブ電極類、又、パリレンなどの柔軟な材料を用い、流路構造などを付加したものなど、多様な電極が開発されてきているが、チャンネル数や柔軟性や生体適合性を含めた材料の問題、インピーダンスの問題など、長期の安定した使用にはまだ多くの問題が残っている。又、末梢神経用の電極に関しては、以前から研究されている神経再生型電極などの他に、近年、LIFE(Longitudinal Intra-fascicular Electrode) や FINE(Flat Interface Nerve Electrode) などが考案・開発され、これらを用いた外部機器の制御も行われている。

紙面のスペースの関係で、神経信号のコーディング・デコーディング則の問題については、割愛したが、シンポジウムではこの点についても議論したい。

Key words: BMI, BCI, MEMS, electrode

32nd Annual International Conference of the IEEE EMBS
Buenos Aires, Argentina, August 31 - September 4, 2010

# OPTIMIZING THE DIAMETER OF HOLES FOR FLEXIBLE REGENERATION MICROELECTRODE

*Riho Gojo[1], Harukazu Saito[3], Takafumi Suzuki[2], Kunihiko Mabuchi[1,2]*
[1]Dept. of Advanced Interdisciplinary Studies, Grad. School of Engineering, The University of Tokyo,
[2]Dept. of Information Physics & Computing, Grad. School of Info. Sci. & Tech., The University of Tokyo
and [3]National Hospital Organization Murayama Medical Center, JAPAN,

## ABSTRACT

In this study, we suggest a new guideline for regeneration microelectrode to be implanted between the severed stumps of peripheral nerves, the microelectrode designed particularly for connecting the signal line of an artificial hand directly to the nerve system. The nerve regeneration microelectrode is an interface device expected to realize a BMI (brain-machine interface).

As the microelectrode device consists of a parylene cable and gold electrodes, it has good flexibility and biocompatibility. The advantage of this technique is that the electrode is in position to make continuous measurements throughout the regeneration process. On the tip of the device, holes are patterned with rounded gold electrodes, where a nerve fiber is growing and passing through each hole during regeneration. By using this unique technique, we can avoid damaging a nerve fiber and make to stable measurement in the long term.

We optimized the diameter of the holes located on the device. Furthermore, since the electrode is fully integrated into a nerve bunch, we can both stimulate the nerve cells by applying a voltage pulse to the motor nerve and take sensory nerve measurements. With this extent of control, we can also selectively measure the signals from these nerve fibers.

## 1. INTRODUCTION

When a peripheral nerve fiber is severed or badly damaged, the body begins to repair the damaged region between the two nerve stumps with different processes from specific directions. Initially, the end of the distal region begins a process called Wallerian degeneration where the end of the distal nerve begins to break down, while simultaneously forming a fibrinous bridge; this bridge is made from fibrin and eventually links the two nerve stumps. It is believed that axon growth is inhibited until this bridge reaches the proximal nerve stump. Once connected, by the bridge, axons begin to grow down along it towards the distal nerve stump [1].

Measuring the current from single nerve cells is extremely difficult due to the inability to isolate individual cells and because of the difference of the length-scale between the cells and the electrodes. However, a microfabricated electrode presents a unique opportunity to isolate individual nerve cells and measure current through them, as explained here: Each regenerating nerve cell must grow linearly to bridge the gap between the severed stumps during nerve fiber regeneration. Therefore, by placing a microfabricated electrode in the path of regenerating nerve cells, we can isolate individual cells and measure the current through them once the nerve fiber has healed. By placing a microfabricated electrode in the path of the regenerating nerve cells, we can isolate individual cells and measure the current through them once the nerve fiber has healed.

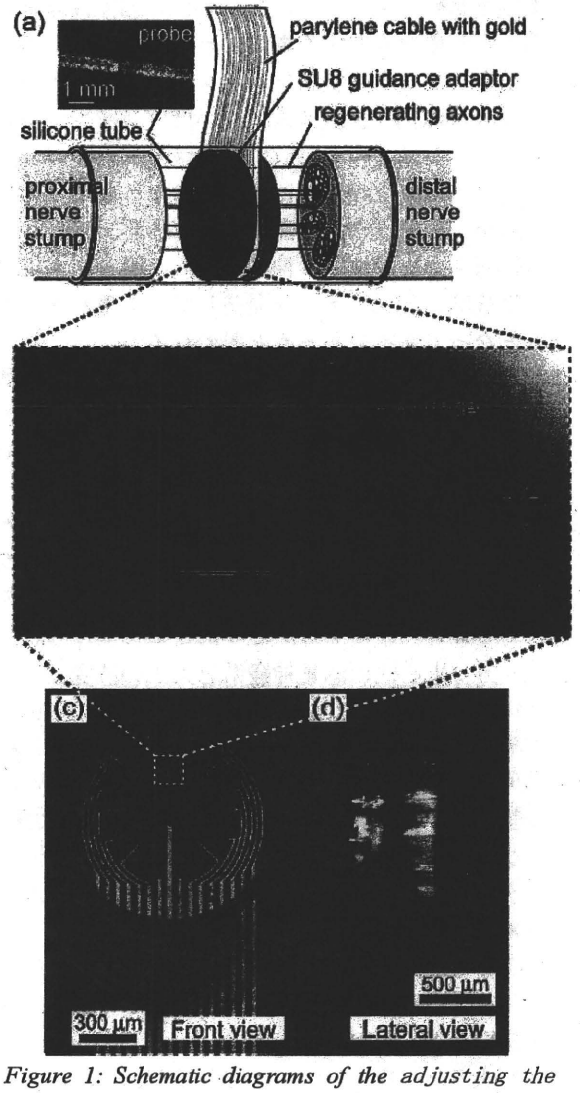


*Figure 1: Schematic diagrams of the adjusting the diameter probe. (a) We designed a probe with 16 micrometer-sized holes in order to direct regenerating axons at a severed gap of stumps through the holes. (b) Hole at recording site for the regenerating axons, to selectively study cell growth by adjusting the hole diameter. (c-d) Photographs of the fabricated probe.*

The advantage of this technique is that the electrode is in position to make continuous measurements throughout the regeneration process. Furthermore, since the electrode

is fully integrated into the nerve bunch, we can both stimulate the nerve cells by applying a voltage pulse and take long-term measurements.

The sieve enables nerve fibers to regenerate through metalized holes; these holes serve as the electrodes. However, since these sieve electrodes are 2D, they provide no guidance for nerve cells that reach a region of the electrode without holes. The cells simply grow randomly and find the holes by chance. In addition, since these electrodes and cables are made from hard materials such as silicon and glass [2-3] because the devices is bigger than the target nerve, the possibility that it may damage the surrounding tissue is high.

At IEEE MEMS 2009, we presented a technique to fabricate an electrode capable of simultaneously enabling current measurements and application of stimulation to nerve cells during and after nerve cell regeneration (Fig. 1) [4].

However, so far, no research has been conducted on determining a suitable hole diameter. We consider that the hole diameter affects the accuracy and sensitivity of measurement on the nerve regeneration process. If the hole diameter is larger than that of the nerve fiber, the nerve regeneration is quick and well; however, detecting a signal will be difficult because the electrode dose not completely contact the nerve. On the other hand, in the case of a smaller hole diameter, the nerve fiber may not pass through the holes. Once the nerve has grown and passed through the holes on the device, it will be possible to obtain signals from the nerve without noise. In order to determine a suitable hole diameter, we fabricated five devices, each with a particular hole diameter, and compared signal responses after the implantation of these devices.

Here, we suggest a new guideline for a regeneration microelectrode to be implanted between the severed stumps of axons.

## 2. DESIGN AND FABRICATION

### Target nerve

We focus on the sciatic nerve in rats because it is a useful nerve to target as it controls the manner in which a rat walks. A normal rat walks on its toes; however, if the sciatic nerve is severed, it begins to walk flat-footed. Upon recovery of the sciatic nerve, it once again begins to walk normally. We can perform a walking track analysis of rats to evaluate the function of their peripheral sciatic nerve, [5] and as a result, we can confirm whether it has healed without operating.

### Fabrication Process

Our flexible probe comprises a thin biocompatible polymer film (parylene) with 16 holes, within which we encase an electrode [6-7] (Fig. 2).

The fabrication procedure is as follows: We first pattern a gold layer on a thin parylene film (Fig. 2(a) and (b)). The thickness of the gold layer is 400 nm. Gold and parylene are patterned with a photoresist (S1818) by standard photolithography. Next, we deposit and pattern a second parylene film (Fig. 2(c–e)). Each parylene film is 20-μm thick. Peel off the electrode from the wafer (Fig. 2(j)). Finally, we complete the process by fabricating the guidance holes on the other side (Fig. 2(k-l)).

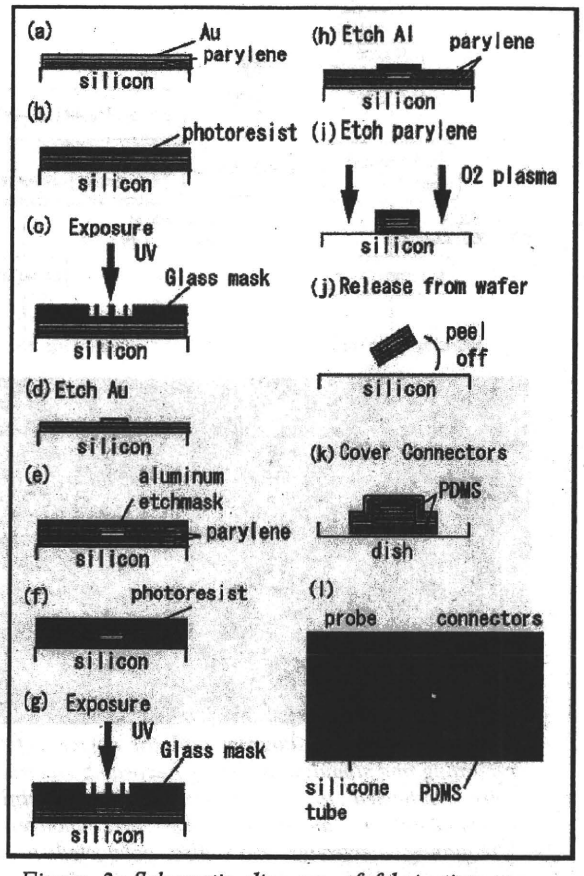


*Figure 2: Schematic diagram of fabrication process. (a-b) First, a gold layer was patterned on a parylene film; then, (c-e) the second parylene film was deposited and patterned. (f-i) an electrode was fabricated with $O_2$ plasma, and (j) it was peeled off from the wafer. (k) Finally, the process is completed by fabricating the connectors with PDMS.*

### Selectivity through Probe Design

Five electrodes have been fabricated, each with a different hole diameter (20, 40, 60, 80, or 100 μm), so as to compare and optimize the hole size for stimulating and nerves and recording nerve signals; the nerves are typically 10 to 20 μm in diameter.

## 3. EXPERIMENTAL RESULTS

The sciatic nerve was cut and led into a silicone tube. Two months after the implant, afferent and motor signals were recorded. The signals recorded using devices with a hole diameter (Φ of 80 μm tended to be clear (Fig. 4), although a slight difference was found in afferent and motor signals. In addition, the signals recorded from the right hind leg were weaker than those recorded from the left hind leg.

Different levels of recovery of the function were observed depending on the diameter of the holes on the electrode section. Devices with a hole diameter larger than

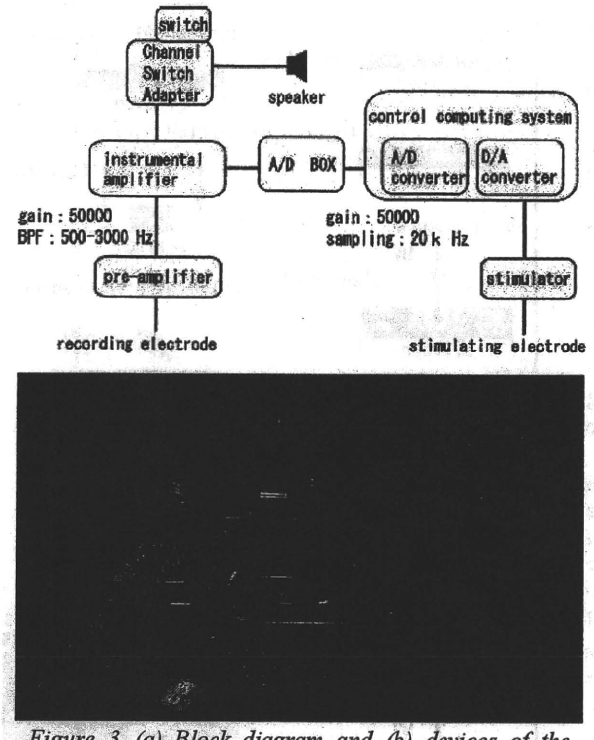


*Figure 3 (a) Block diagram and (b) devices of the recording and stimulating system. Recording electrodes were connected to a computer via pre-amplifier, instrumentation amplifier, and A/D converter. Stimulating electrodes were also connected to the computer via D/A converter and stimulation device.*

Φ60 μm seemed to produce a high level of recovery, while those with hole Φ20 μm led to only a small level of recovery. As showed in Fig. 5, ulcers formed on the toes of the

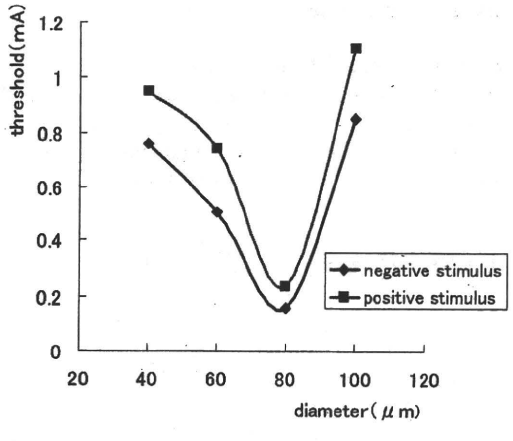


*Figure 4: Minimum currents (threshold) to induce a stitch in a hind limb with various diameters of electrode holes.*

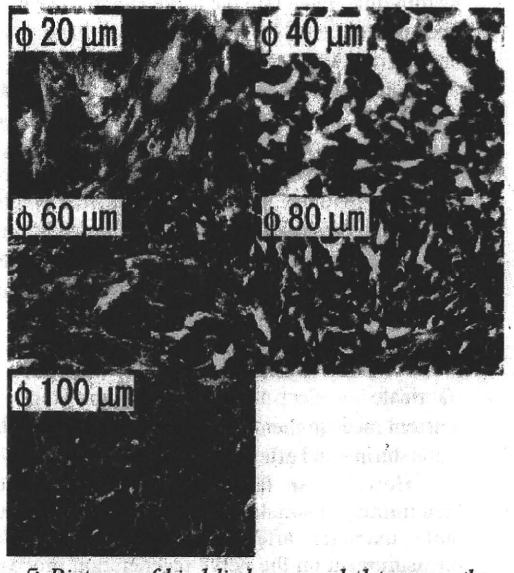


*Figure 5: Pictures of hind limbs, recorded two months after the implants. Side view on the left and bottom view on the right. Arrows show ulcers formed on the skin.*

stimulated legs when devices with holeΦ40–80 μm were used. This result may indicate that the rats had unusual perception owing to incomplete restoration of nerve fibers.

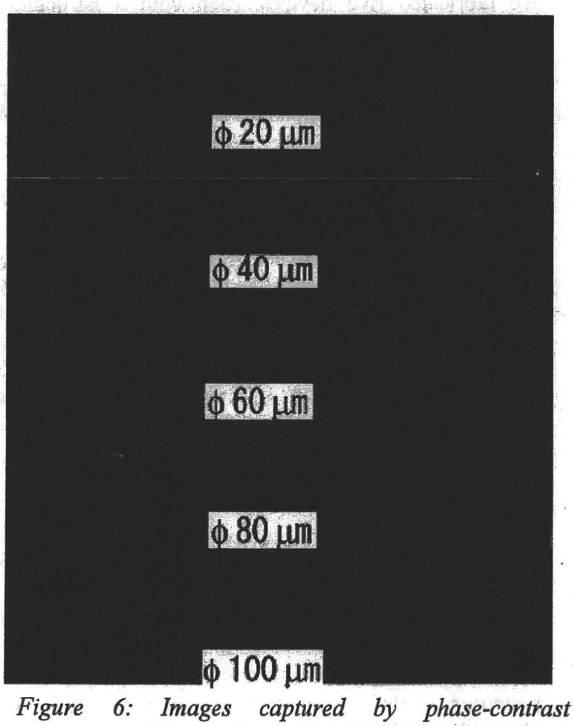


*Figure 6: Images captured by phase-contrast microscopy. The proximal side of the electrode is sliced in the vertical direction. Red: anti-MBP antibody, Blue: antineurofilament antibody.*

The sciatic nerves containing the electrodes were resected and were fixed by 4% paraformaldehyde and frozen sectioned (Fig. 6). The sections were stained with an antineurofilament antibody and an anti-MBP (myelin basic protein) antibody. The regeneration axons of Φ20 μm were few in the case of pigmentation with the antineurofilament antibody on the distal side of the electrode, and a large number of regeneration axons with Φ40 μm or more were admitted. Further, numerous parts

with comparatively large positivity and Φ40 μm or more were observed, though they lay scattered in small parts of Φ20 μm in the dye with the anti-MBP antibody. It was considered that the c with a large diameter and containing a marrow fiber had regenerated through the electrode and formed these parts of Φ40 μm or more.

We found that the threshold to induce a stitch in a limb depends on the diameter of holes on the microelectrode device (Fig. 4). The minimum value of the threshold was obtained to be 0.2 mA with a hole of Φ80 μm. We observed ulcers on the toe of the stimulated legs, particularly in the case of hole diameters ranging from Φ40 μm to Φ80 μm.

## 4. CONCLUSION

In summary, we propose a regeneration-type electrode that represents important advances over the present neural electrodes. By considering the overall results, we conclude that a hole diameter of 80 μm is suitable for facilitating nerve regeneration and performing sensitive measurement.

Our future plan is to integrate multiple electrodes having holes of a suitable size into this flexible device so as to perform multi-channel measurement.

## REFERENCES


[1] Y.-C. Lo, *et al.*, Neural guidance by open-top SU-8 microfluidic channel, *IEEE MEMS*, Maastricht, January, pp. 671-674, 2004.

[2] W.L.C. Rutten, Selective electrical interfaces with the nervous system, *Annu. Rev. Biomed. Eng.*, vol. 4, pp. 407-452, 2002.

[3] T. Akin, *et al.*, A micromachined silicon sieve electrode for nerve regeneration applications. *IEEE Trans. on BME.*, vol. 41, pp. 305-313, 1994.

[3] R. Gojo, *et al.*, A flexible regeneration microelectrode with CELL-GROWTH GUIDANCES, *IEEE MEMS*, Sorrento, January, pp. 256-259, 2009.

[4] T. Suzuki, *et al.*, Flexible microelectrode for interfacing regenerating peripheral nerves, Proc. of 19th International *IEEE EMBS.*, 1997 (CD-ROM).

[5] G. M. T. Hare, *et al.*, Walking track analysis: a long-term assessment of peripheral nerve recovery. *Plast Reconstr Surg*, vol. 89, pp. 251-258, 1992.

[6] T. Suzuki, *et al.*, Flexible microelectrode for interfacing regenerating peripheral nerves, Proc. of 19th International *IEEE EMBS.*, 1997 (CD-ROM).

[7] S. Takeuchi, *et al.*, 3D Flexible multichannel neural probe array, *Journal of Micromechanics and Microengineering*, vol. 14, pp. 104-108, 2004.

32nd Annual International Conference of the IEEE EMBS
Buenos Aires, Argentina, August 31 - September 4, 2010

# RatCar: A vehicular neuro-robotic platform for a rat with a sustaining structure of the rat body under the vehicle

Osamu Fukayama, *Member, IEEE*, Takafumi Suzuki, *Member, IEEE*, and Kunihiko Mabuchi, *Member, IEEE*

***Abstract*— An online neuro-robotic platform in the form of a small vehicle, the "RatCar" has been developed. First, a rat had neural electrodes implanted in the motor cortices to record extracellular potentials. Then, our system combined the rat and its vehicle body by hanging the rat under its floor. In this paper, an experimental platform is proposed to observe and analyze motor commands by correlating neural signals with locomotion states. It was designed to operate in 2 modes; (a) adaptively correlating neural signals and locomotion states to determine motor commands, and (b) applying the estimated motor commands to control the vehicle according to the intention of the rat. As a result, time-varying correlation between neural and locomotion activities has been adaptively visualized in real time to analyze motor commands in various body conditions. In addition, a control of the vehicle has been improved.**

## I. INTRODUCTION

Brain-machine interfaces (BMIs) are currently of interest because of their ability to provide a new modality for devices control. While a number of applications are already tested on human beings using non-invasive measurement of brain activity such as the electroencephalogram (EEG), direct recording of the extracellular potentials is a promising technique to extract motor commands to control artificial devices more precisely. Chapin et al [1], for example, developed a system to control the movement of a robotic arm using the neural signals from the primary motor cortex of a rat. More complex control of a robot arm through the neural signals of monkeys were reported by Wessberg et al. [2].

Our BMI system is in the form of a small vehicle, which we call the "RatCar". It is unique in that a neural signal source (i.e., a rat) is integrated inside the device (i.e., the vehicle body) and the whole components move around. The rat is therefore provided with direct visual and sensory feedback as the vehicle moves. We expect that this condition enables the rat's brain to modify itself adapting to the vehicle system. Our ultimate goal is to let the vehicle collaborate with the brain to achieve a locomotion as the rat intended on behalf of natural limbs.

A rough estimation of the locomotion according to neural signals had been achieved in the past study by the authors [3] to determine the movement of the vehicle. In this paper, the vehicle form was revised by elevating the floor higher to hang a rat under the vehicle body. Its shape placed a rat closer to the ground so that it was capable of exploring the ground freely. It also enabled a "passive" control mode of the vehicle. In this mode, the vehicle was neutralized by detaching motors, and a rat was trained to tow the vehicle. Correlation parameters representing motor commands were compared in various situations.

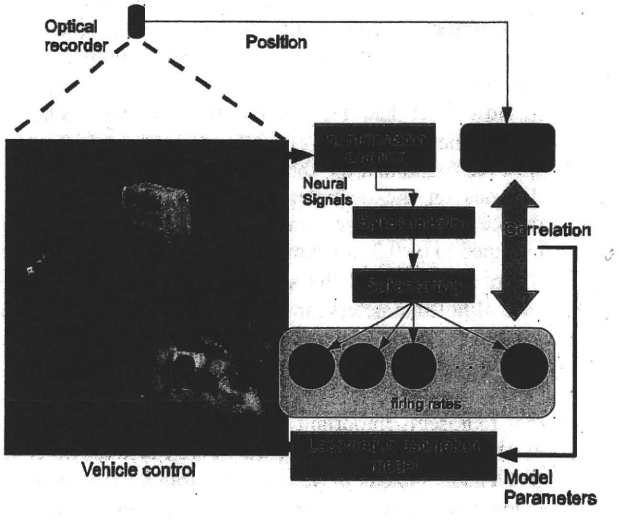


Fig. 1. Block diagram of the RatCar system. The vehicle to move around on a field holding a rat, recorders for neural signals and locomotion states, and a locomotion estimation model to determine vehicle movements are connected.

## II. METHODOLOGY

Our system consists of the vehicle to move around on an experimental field (2 m × 1 m), simultaneous recorders for neural signals and locomotion states, and a locomotion estimation model which correlates those two acquired values in real time to determine vehicle movements (Fig. 1).

### A. Neural Signals Recorder

*1) Implant:* Neural electrodes have been fabricated with MEMS technology to acquire extracellular multiunit activities (MUA). Each electrode had 4 gold recording sites on a thin soft layer made of parylene polymers (Fig. 2a). Then, a small connector (1 mm - pitch IC socket) was attached to connect the lines to an amplifier.

This work was supported by Grant-in-Aid for Scientific Research (Y-Startup) 30508205 and (A) 20246045 from the Ministry of Education, Culture, Sports, Science and Technology of Japan and by Grant-in-Aid for Research on Advanced Medical Technology H17-Nano-010 from the Ministry of Health, Labour and Welfare of Japan.

All the experiments we performed followed guidelines given by the "Animal Experiments Committee of the University of Tokyo".

The authors are with Graduate School of Information Science and Technology, The University of Tokyo, 7-3-1 Hongo, Bunkyo, Tokyo, JAPAN of@ratcar.org

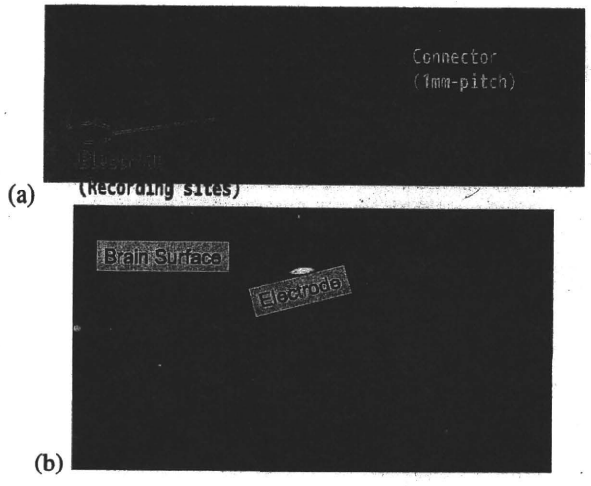


Fig. 2. (a) A fabricated electrode which has 4 recording sites on a tip and a connector on the other end. (b) Electrodes implanted in the brain penetrating the surface. Dura mater had been removed in advance.

They were implanted in the motor cortical regions of 8 male Wistar rats (Fig. 2b) according to a stereotaxic atlas [4] and functional localization maps [5], [6].

*2) Signal Acquisition:* Neural signals were derived by differentiating potentials between 3 recording sites and 1 reference site on each electrode. They were then amplified and filtered (Gain: 5,000, BPF: 500 - 5,000 Hz) by *Multichannel Systems PGA-64* or *FA-64* followed by an A/D converter (*National Instruments PCI-6071E*, 20 kSps for each channel) installed in a personal computer.

*3) Spikes Detection and Sorting:* Neural firing sequences $\vec{s}_t$ were detected as the recorded waveform showed local maximal or minimal values. Note that either positive or negative peak were counted as neural firings because of the differential recording setup.

Then, a Gaussian-mixture model (GMM) sorted the distribution of detected spikes $z_t$ into classes representing $n$-th neuron ($n = 1, \ldots, N$) respectively. Each neuron were assumed to generate spikes with a constant peak amplitude $\mu_n$ distributed by a Gaussian $N(\mu_n, \sigma_n^2)$ ($\mu_n$: mean, $\sigma_n^2$: variance). Consequently, the distribution of peak amplitudes $P(z)$ were described as

$$P(z) = w_n N(z;\, \mu_n, \sigma_n^2), \tag{1}$$

where $w_n$ is a prior probability of each Gaussian.

The expectation-maximization (EM) algorithm[7] estimated the parameters $w_n, \mu_n, \sigma_n^2$ for the GMM while a number of Gaussians were determined by searching maximum likelihood of GMM as increasing the number. Finally, a class $n$ to give a maximum probability $P(z|n)$ to generate a spike $z_t$ were chosen.

### B. Locomotion Recorder

An optical position tracker (*KEYENCE CV-5700*) was installed over the experimental field. The system captured an image in 1024 × 768 resolution every 100 ms to detect positions of 4 colored markers. While 2 markers were placed on the back of each rat (Fig. 3), the other 2 markers were placed on the vehicle. Velocity (Fig. 4(a)) and directions of the rat and the vehicle were calculated according to temporal changes and relative positions (Fig. 4(b)) of those markers.

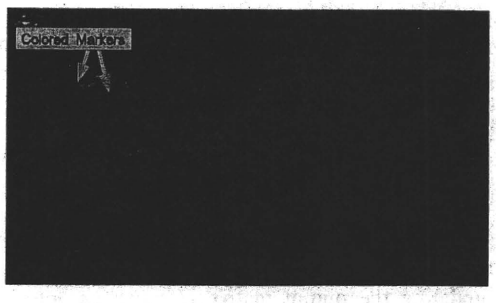


Fig. 3. A rat with markers placed on the back. A white jacket and a black belt was used to combine the rat with the vehicle.

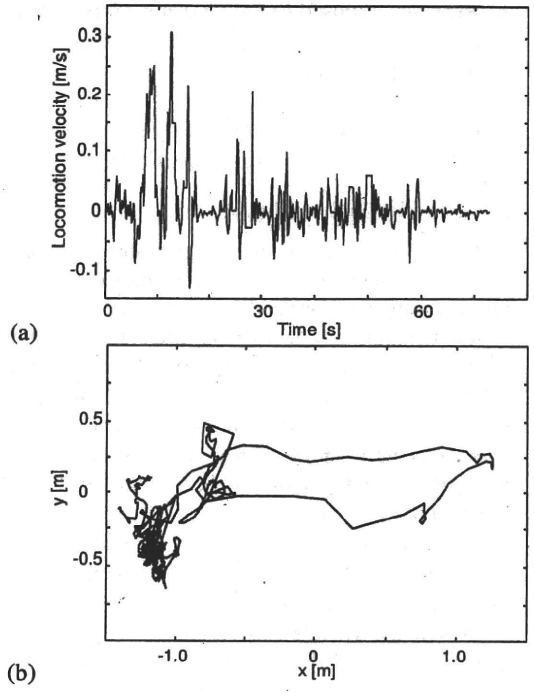


Fig. 4. An example of (a) locomotion velocity and (b) trajectory of a rat recorded with the optical position tracker.

### C. Locomotion Estimation

*1) Correlation Model:* A state space model as described in equation (2),(3) correlated the neural firing rates $\vec{y}(p)$ and a locomotion states $\vec{x}(p) = (x_{\text{velocity}}(p),\ x_{\text{azimuthal variation}}(p))^{\mathrm{T}}$ (a velocity and azimuthal variation) at $p$-th bin every 100 ms;

$$\vec{x}(p+1) = F\vec{x}(p) + \vec{\xi}(p) \tag{2}$$

$$\vec{y}(p) = H_p\vec{x}(p) + \vec{\eta}(p) \tag{3}$$

where the state transition matrix $F$ and output matrix $H_0$ were initially tuned for each subject in the first trial so that the estimation result or vehicle should not go out of control.

Here, the Kalman filter algorithm were applied to the model to estimate the locomotion states $\hat{\vec{x}}(p)$ by sequentially acquired neural firing rates $\vec{y}(p)$:

$$\hat{\vec{x}}(p+1) = F(I - K_p H_p)\hat{\vec{x}}(p) + FK_p\vec{y}(p). \quad (4)$$
($K_p$ : Kalman gain)

*2) Online Update of Parameters:* Meanwhile, an observation update algorithm of the Kalman filter are capable of updating the output matrix $H$ when an actual locomotion states were provided as a teaching source.

Assuming the neural firings sequence were orthogonal, the $H$ were decomposed to the elements corresponding to each neuron $n$ (i.e., $H = (\vec{h}_{n,p}) = (h_{n1,p},\ h_{n2,p})$) and they were updated individually:

$$\hat{\vec{h}}_{n,p+1} = (I - K_{n,p}\vec{x})\hat{\vec{h}}_{n,p} + K_{n,p}\vec{y}(p). \quad (5)$$
($K_{n,p}$ : Kalman gain for each neuron $n$)

### D. Vehicular Body and Control

According to the estimated locomotion velocity and azimuthal variance, the vehicle which had a high-floored structure hanging a rat under the floor was controlled to trace the actual movement of the rat. The control operated in 2 modes; a "passive" mode and a "neuro-robotic" mode. In the passive mode, the motor driver of the vehicle was neutralized and the rat was loosely binded to the vehicle body towing it. In the neuro-robotic mode, the rat was sustained under the vehicle floor by the jacket and belt (Fig. 3) so that its limbs gently touched the ground.

In this paper, those modes were applied to compare neural activities in 3 situations; natural locomotion (by the own limbs of a rat), half-robotic locomotion (passive mode; a rat towed the vehicle), and full-robotic locomotion (neuro-robotic control of the vehicle hanging a rat).

## III. RESULTS AND DISCUSSION

### A. Parameters Update

In an initial period of each trial, a rat was left on the field and freely moved around. The correlation parameters that we initialized with 0.0 were updated, and they converged in less than 40 seconds on most trials. A typical result is shown in Figure 5(a).

Then, the rat was binded with the vehicle and motivated to move by an experimenter blowing on its back. As a result, the parameters showed remarkable changes as the rat started moving with the vehicle, then they fell into another converged states (Fig. 5(b)).

Finally, the rat was moved by the vehicle in the neuro-robotic mode. In this situation, the parameters were updated using the correlation between neural firings and actual movement of the vehicle. The parameters should be kept converged if the estimation of the vehicle control had been proper. Those results were observed widely on any rats although the converged values was different for each subject.

The fact that the parameters converged in 40 seconds during the free locomotion suggests that our simple model

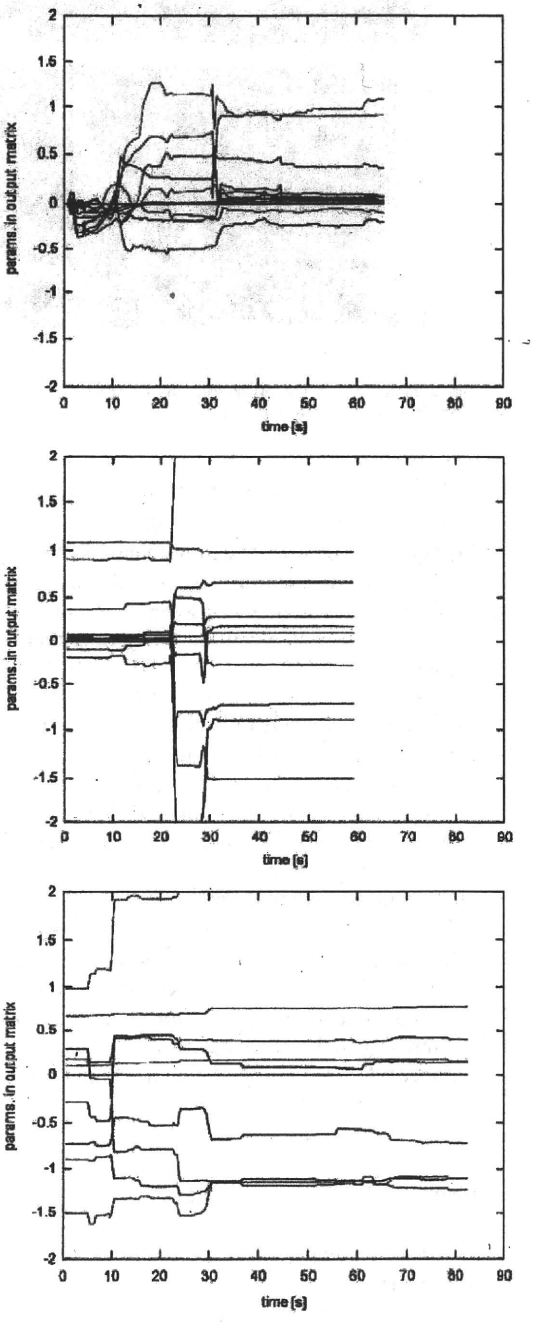


Fig. 5. Adaptively updated correlation parameters (elements of output matrix $H$) observed (a) as a rat freely moved on the field in an initial identification period, (b) as a rat towed the vehicle, (c) as a rat was moved by the vehicle in neuro-robotic mode.

were applicable to describe motor commands. Then, as the rat was binded with the vehicle, the most parameters increased. It is reasonable because the rat brain should send stronger motor commands to muscles to move the vehicle and its original body as a whole.

However, neuro-robotic control of the vehicle resulted in sudden variation of the identified parameters which should be unchanged if a proper motor commands representation was realized by our model. Some pairs of 2 parameters were passing each other (typically on 10 seconds from the start point in Fig. 5(c)), which may suggest an improper spike sorting.

### *B. Vehicle-Rat Integration*

The system was capable of holding a rat under the vehicle floor, and the rat looked relaxed as long as the vehicle was neutralized (in passive mode). Weight of the whole vehicle was less than 1 kg and a rat (varied from 300 g to 500 g in weights) was able to tow the vehicle on a flat field.

In the neuro-robotic mode, the motors which were sealed inside the body succeeded in not making the rats frightened as the vehicle gently moved. Most rats (6 out of 8) were tamely hanged under the vehicle, although 2 of them became hyperactive to turn down the whole system.

### *C. Future Direction*

Another problem with our current system is that we cannot compare an estimated movement of the vehicle to real intention of a rat in neuro-robotic mode, because the rat was forcibly moved with the vehicle even if it tried to move to other direction. A force measurement device should be attached to the belt binding a rat body and the vehicle so that the motion errors between those two are measured.

## IV. CONCLUSION

In this paper, a neuro-robotic platform has been proposed to observe and analyze motor commands by comparing correlation between neural signals and locomotion states in various situations. It is capable of applying other electrodes or motor decoders to find out a better methods to realize precise brain-machine interfaces.

## REFERENCES


[1] J. K. Chapin, K. A. Moxon, R. S. Markowitz, and M. A. Nicolelis, "Real-time control of a robot arm using simultaneously recorded neurons in the motor cortex," *Nature Neuroscience*, vol. 2, no. 7, pp. 664 – 670, 1999.

[2] J. Wessberg, C. R. Stambaugh, J. D. Kralik, P. D. Beck, M. Lauback, J. K. Chapin, J. Kim, S. J. Biggs, M. A. Srinivasan, M. A. L. Nicolelis, "Real-time prediction of hand trajectory by ensembles of cortical neurons in primates," *Nature*, vol. 408, pp. 361 – 365, 2000.

[3] O. Fukayama, N. Taniguchi, T. Suzuki, K. Mabuchi, "RatCar System for Estimating Locomotion States using Neural Signals with Parameter Monitoring: Vehicle-formed Brain-Machine Interfaces for Rat," *Proc. 30th Annual International IEEE EMBS Conference*, pp. 5322 – 5325, 2008.

[4] G. Paxinos and C. Watson, The Rat Brain in Stereotaxic Coordinates, Compact Third Edition. Academic Press, 1997.

[5] R. D. Hall and E. P. Lindholm, "Organization of Motor and Somatosensory Neocortex in the Albino Rat," *Brain Research*, vol. 66, pp. 22 - 38, 1974.

[6] S. P. Wise and J. P. Donoghue, Motor cortex of rodents. *Motor Cortex*, Plenum Press, 1984.

[7] A. P. Dempster, N. M. Laird, D. B. Rubin, "Maximum Likelihood from Incomplete Data via the EM Algorithm," *J. R. Stat. Soc. Ser. B*, vol. 39, no. 1, pp. 1 – 38, 1977.

32nd Annual International Conference of the IEEE EMBS
Buenos Aires, Argentina, August 31 - September 4, 2010

# Estimation of finger postures to control a maniform device for playing a trumpet using electromyographic signals with external triggers

Yutaro Kobayashi, Osamu Fukayama, Takafumi Suzuki, and Kunihiko Mabuchi

*Abstract*—**Electromyographic (EMG) signals have been used to control active prosthetic arms for amputees. One of the obstacles in making such prosthetic arms is the *timed estimation of posture*, because EMG signals and muscle movements are not necessarily synchronized. We estimated the finger motions for trumpet players by using both surface EMG (sEMG) and the timing information using body motion. The algorithms consisted of Principal Component Analysis (PCA), and Support Vector Machine (SVM). The results showed that applying the timing information using body motion increases how precisely the motion of the fingers is estimated.**

## I. Introduction

Electromyographic (EMG) signals have been used to control active prosthetic arms for amputees. One of the obstacles in creating such prosthetic arms is the *timed estimation of posture* because EMG signals and muscle movements are not necessarily synchronized (Fig. 1(a)). Therefore, the precision of posture estimation can be significantly improved by externally providing timing information using body motion. An experimental system for playing the trumpet with surface EMG (sEMG) signals to show the validity of our claim has been developed and shown as Fig. 1(b). The system recorded sEMG signals from the forearm muscles of trumpet players. The postures of the hands that push the trumpet valves were estimated using the sEMG signals while the correct timing in which the valves were pushed was externally provided.

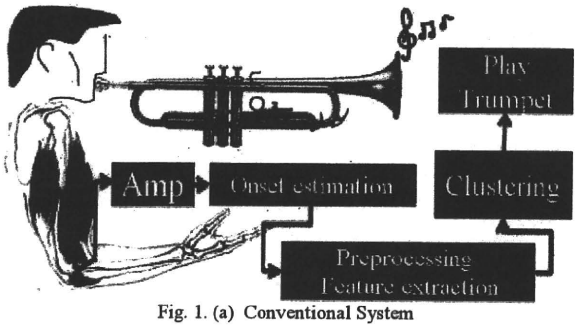


Fig. 1. (a) Conventional System

Manuscript received April 23, 2010.

Y. Kobayashi, O. Fukayama, T. Suzuki, and K. Mabuchi are with Graduate School of Information Science and Technology, the University of Tokyo, Tokyo, Japan(phone: 81-3-5841-6880;
e-mail: Yutaro_Kobayashi@ipc.i.u-tokyo.ac.jp ).

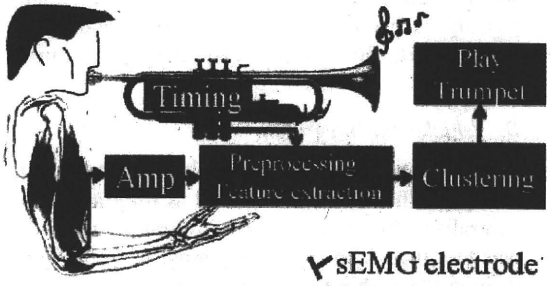


Fig. 1. (b) Proposed System

### A. Motor Neurons and Muscles

Brains transmit motion orders to axons of upper motor neurons inside brains, and then to spinal cords. These orders are then transmitted through the synapses of lower motor neurons. Axons of the lower motor neurons become peripheral nerves and make synapses with muscle fibers. All the corresponding muscle fibers that a single motor neuron innervates are called the *motor unit*. There are over 1000 muscles controlled by a single motor neuron. When the orders reach the muscles, the muscles contract and the EMG signal is recorded.

### B. EMG and Motor Unit Recruitment

Motor unit recruitment is defined as "the successive activation of the same and additional motor units with increasing strength of voluntary muscle contraction" [1]. Muscles use the recruitment process to generate various types of forces. The central nervous system increases the strength of muscle contractions by the following steps.

(A) Increase the number of motor units
(B) Increase the firing rate of each motor unit

At lower levels of muscle contraction strength, step (A) is prominent. However at the same time, step (B) is also observed which explains the complexity of motor recruitment.

There is also a recruitment sequence for different types of motor units: S(Slow), FR(Fast, Resistant), and FF(Fast, Fatigable) are the three main types of motor units and are recruited in the sequence of S, FR, and FF. Addition to the recruitment sequence, larger muscle contraction strength is generated by increasing the firing rate of motor units. Even if the subject makes a specific motion, the muscles near the target areas of the electrodes may only generate a feeble sEMG signal. This causes the difficulty in detecting the *onset* timing when dealing with sEMG signals[2][3].

### C. General Characteristics for Playing the Trumpet

Trumpet players make different pitches by pushing the 3 valves in different patterns with the right hand. The 2nd finger controls the 1st valve (the valve closest to the mouthpiece), and the 3rd and 4th finger control the 2nd and 3rd valve respectively. There are 6 patterns in which the valves can be pushed and are musical are shown in Figure 2. Surface EMG signals were recorded to estimate the postures of the three fingers. The correct timing in which the valves were pushed was also recorded (timing is given externally).

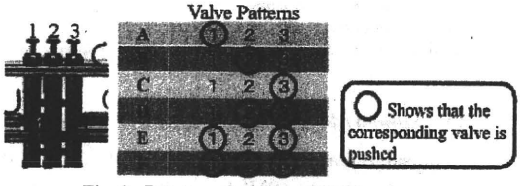


Fig. 2. Patterns of pushing trumpet valves

## II. METHODS

### A. Onset Detection Method

The selected threshold-based onset detection method [3], proposed by *Hodges and Bui*, has the characteristics for high onset detection rate and can be used for high onset detection. This method is used to estimate the timings of the valves pushed from sEMG signals. Equation 1−3 show how the onset is detected.

Here $\overline{\upsilon}_0$ shows the average of the first $M$ data, $\overline{\sigma}_o$ shows the standard deviation of the first $M$ (200) data, $W$ shows the moving average of 5000 data, $M$ shows the number of data used to calculate $\overline{\sigma}_o$, $\overline{\upsilon}_0$, $t_a$ represents the estimated onset time, and $h$ show the threshold (2.5).

$$t_a = \min\{k \geq W : g_k \geq h\} \tag{1}$$

$$g_k = \frac{1}{\overline{\sigma}_o}(\tilde{y}_k - \overline{\upsilon}_0) \tag{2}$$

$$\tilde{y}_k = \frac{1}{W}\sum_{i=k-W+1}^{k} y_k \tag{3}$$

The results were then used to compare with the actual valve pushed timings in section VI A, B.

### B. Timing Information Provided Externally

The valve pushed timings were measured in two different methods. The first method measured the valve pushed timings by placing sensors onto the valves. The second method measured the timings of the breath by placing a vibration sensor onto the mouthpiece. In this experiment, the results of the first method were used as *timing information provided externally* for the simplicity.

### C. Feature Extraction and Electrode Placement

Eight sEMG electrodes were applied to the subjects' right forearms (Fig. 3), and recorded with the sampling rate of 25 kHz. We extracted 0.16 second of data, right before the valves were pushed, was extracted. Covariance matrices were then calculated and used as features.

Electrode CH1 and 2 were placed on the extensor digitorum muscle to measure the flexion of all fingers. Electrode CH3 was placed on the flexor carpi radialis muscle to measure wrist movement. Electrode CH4 was placed on extensor indicis to detect the movement of the 4th finger. Electrode CH5 and 8 were placed on flexor carpi ulnaris muscle to detect the movement of the 4th finger. Electrode CH6 and 7 were placed on flexor digitorum superficialis muscle to detect the movement of 2nd and 3rd fingers respectively.

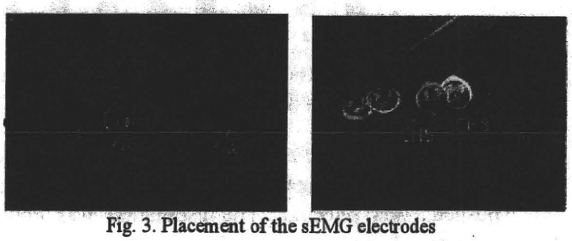

Fig. 3. Placement of the sEMG electrodes

## III. EXPERIMENT

### A. Experiment I

Two subjects were asked to push the valves with the instructions of the following subsets.

(a) Push 1st valve *10 times (valve pattern A)
(b) Push 2nd valve *10 times (valve pattern B)
(c) Push 3rd valve *10 times (valve pattern C)
(d) Push 2nd, and 3rd valves *10 times (valve pattern D)
(e) Push 1st, and 3rd valves *10 times(valve pattern E)
(f) Push 1st,2nd, and 3rd valves *10 times (valve pattern F)

### B. Experiment II

Two subjects (K, Y) were asked to push the valves with the instructions of the following subsets. Note that only valve patterns A, B, C have been conducted by the subjects.

(a) Push 1st valve *30 times (valve pattern A)
(b) Push 2nd valve *30 times (valve pattern B)
(c) Push 3rd valve *30 times (valve pattern C)
(d) Push 2nd, and 3rd valves *30 times (valve pattern D)
(e) Push 1st, and 3rd valves *30 times(valve pattern E)
(f) Push 1st,2nd, and 3rd valves *30 times (valve pattern F)
(g) Push 1st, 2nd, 3rd valve 10 times each in this sequence
(h) Push 1st, 2nd, 3rd valve randomly for 30 times
(i) Push all patterns randomly for 50 times

## IV. RESULTS

### A. Precision of Onset Detection Methods

The selected threshold-based onset detection method [3] was used to estimate the timings needed to push the valves from the 8 sEMG signal of each of the electrodes. The estimated number of times that valves were pushed (estimated number of times pushed) is shown in Figure 3. The bar lines shows the estimated maximum and the minimum number of times pushed through out Experiment I.